

Stepping Out of Similar Semantic Space for Open-Vocabulary Segmentation

Yong Liu^{1*}, Songli Wu^{1*}, Sule Bai^{1*}, Jiahao Wang², Yitong Wang³, Yansong Tang^{1†}

¹Tsinghua Shenzhen International Graduate School, Tsinghua University

²The University of Hong Kong ³ByteDance Inc.

liuyong23@mails.tsinghua.edu.cn, tang.yansong@sz.tsinghua.edu.cn

Abstract

Open-vocabulary segmentation aims to achieve segmentation of arbitrary categories given unlimited text inputs as guidance. To achieve this, recent works have focused on developing various technical routes to exploit the potential of large-scale pre-trained vision-language models and have made significant progress on existing benchmarks. However, we find that existing test sets are limited in measuring the models’ comprehension of “open-vocabulary” concepts, as their semantic space closely resembles the training space, even with many overlapping categories. To this end, we present a new benchmark named *OpenBench* that differs significantly from the training semantics. It is designed to better assess the model’s ability to understand and segment a wide range of real-world concepts. When testing existing methods on *OpenBench*, we find that their performance diverges from the conclusions drawn on existing test sets. In addition, we propose a method named *OVSNet* to improve the segmentation performance for diverse and open scenarios. Through elaborate fusion of heterogeneous features and cost-free expansion of the training space, *OVSNet* achieves state-of-the-art results on both existing datasets and our proposed *OpenBench*. Corresponding analysis demonstrates the rationality and effectiveness of our proposed benchmark and method.

1. Introduction

Semantic segmentation is one of the most fundamental tasks in computer vision, which targets at assigning semantic category to pixels in an image. Despite achieving excellent progress in recent years [2, 6, 20, 21, 33–36, 38, 42, 49–52, 57], traditional semantic segmentation approaches rely on predefined categories sets and tend to falter when encountering categories absent during the training phase, significantly impeding their real-world application. Such chal-

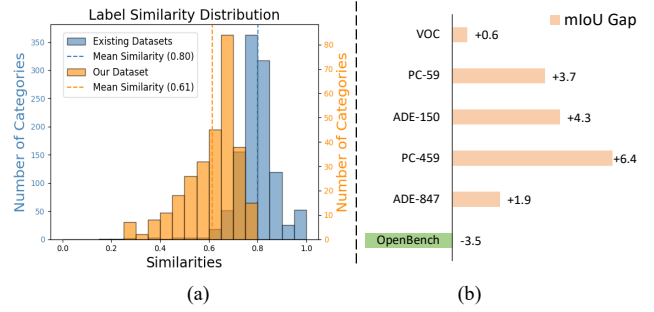


Figure 1. (a) shows the similarity distribution of the existing test set (blue) and our OpenBench (orange) with the training semantic space. (b) illustrates the performance gap between the methods finetuning [10] and frozen [60] CLIP on different benchmarks.

lenge has inspired the exploration of Open-Vocabulary Segmentation (OVS) task [12, 15, 17, 18, 27, 37, 55, 63]. Different from traditional closed-set segmentation, OVS methods aim to segment arbitrary categories under the guidance of given text inputs, which has many potential applications such as auto-driving and human-robot interaction [19, 39].

However, it is challenging to identify unseen categories without the intervention of external knowledge. Therefore, an intuitive idea is to introduce large-scale vision-language model [24, 46] trained with numerous sources to extend the semantic space of segmentation models. Following this idea, existing OVS methods [10, 31, 37, 56, 60, 61] concentrate on exploring how to exploit the pretrained knowledge prior more effectively and derive several technical routes. Early methods [12, 31, 59] adopt a two-stage pipeline. This approach first generates class-agnostic mask proposals with segmentation models, following which the pre-trained CLIP [46] serves as an additional classifier to execute region-level open-vocabulary classification. However, this strategy incurs heavy computation overhead, as it requires repeated forward passes of the CLIP vision encoder for each mask. This can be prohibitively expensive for real-world applications. To address this problem, researchers [25, 60–62] propose to unify classification and segmentation within a shared space, *i.e.*, integrating frozen CLIP features into the segmenter and extracting CLIP embeddings from potential

*Equal contribution

†Corresponding author

target regions to enable simultaneous classification and segmentation. These methods achieve remarkable performance in a more efficient one-stage pipeline. Subsequently, some works [10, 56] discover that finetuning the CLIP encoder could further enhance the model’s performance on existing test sets. They develop an early fusion paradigm based on cost map and achieve outstanding segmentation results. However, this performance boost is somewhat counterintuitive, as fine-tuning CLIP typically adapts it to specific training semantic spaces, which could reduce its original generalization ability. Yet, the ability of generalized visual-linguistic alignment is precisely what the open-vocabulary task requires. So why does fine-tuning CLIP appear to benefit the performance of OVS?

This question drives us to revisit the existing evaluation benchmarks of the cross-dataset evaluation paradigm. We count the maximum similarity of each category in test set to the training semantics. Figure 1 (a) illustrates the similarity distribution of all test categories to the training space (blue color). Results indicate that the existing test data is, in fact, highly similar to the training semantic space. Specifically, even the most challenging ADE-847 [65] and PC-459 [44] datasets have an average similarity to the training classes of 0.79 and 0.83. PC-59 [44] and VOC [13] datasets even have a similarity to the training semantics of 0.95 and 0.97. This explains why finetuning CLIP on training set can lead to further performance gains on existing benchmarks. However, it somewhat conflicts with the purpose of the open-vocabulary setting, which aims to achieve segmentation of unlimited categories in the real world.

To address the above problem and provide a more comprehensive measure of OVS models, we propose a new evaluation benchmark named OpenBench, which is characterized by significant semantic differences from the training data. Figure 1 (a) also demonstrates the similarity distribution of our OpenBench (orange color). It can be seen that our benchmark contains more novel classes compared to the existing test sets. We evaluate the performance of approaches across different technical routes on our benchmark, and the findings diverge from those obtained on existing test sets. As shown in Figure 1 (b), while finetuning CLIP yields steady performance gains on existing datasets, it shows a significant drop on our benchmark. This outcome also supports our motivation for proposing a benchmark that diverges substantially from the training space.

In addition, we also present a framework named OVSNet to improve the segmentation performance for diverse and open scenarios. In OVSNet, we adopt a Proxy Calibration (PC) training strategy to enhance the robustness of model representations by broadening the training space with no additional cost. This strategy leverages the synthesis of proxy embeddings, which approximate unseen semantics through convex combinations of in-vocabulary classes. Addition-

ally, inspired by random walk [16], we propose a gradient-free fusion of CLIP embeddings and segmentation decoder features to model a robust joint space and mitigate potential overfitting issues related to training semantics. With the above proposed designs calibrating model knowledge from the aspects of training space and features separately, our OVSNet demonstrates strong performance across a wide range of scenarios, both on existing test sets similar to the training semantics and on our proposed novel OpenBench. Related ablations also demonstrate the effectiveness and soundness of our proposed strategies.

Our contributions can be summarized as follows:

- We present a new benchmark named OpenBench for OVS, which is characterized by significant semantic differences from the training space. While using it to evaluate the comprehension of OVS methods in more open scenarios, we reach a different conclusion from that of the existing test sets.
- We propose OVSNet to improve the segmentation performance on diverse and open scenarios. It adopts a Proxy Calibration training strategy to broaden training space without additional cost. Besides, a gradient-free algorithm is leveraged to fuse CLIP embeddings and segmentation features for modeling robust joint space.
- Our method achieves state-of-the-art performance on existing benchmarks and the proposed OpenBench. Extensive experiments are conducted to prove the effectiveness and soundness of the proposed algorithms.

2. Related Work

Open-Vocabulary Segmentation. This task aims to segment an image and identify regions with arbitrary given text queries [1, 4, 15, 41, 55]. Pioneering work [55] replaces the output convolution layer by computing the similarity between visual features and linguistic embeddings, which has become common practice. Later, some methods [12, 15, 31, 58, 59] propose a two-stage pipeline: the model first generates class-agnostic mask proposals, then a pretrained CLIP [46] is utilized to perform sub-image classification by cropping and masking corresponding regions. With the combination of both in-vocabulary and out-vocabulary classification, these methods obtain great performance. However, this strategy incurs heavy computation overhead, as it requires repeated forward passes of the CLIP vision encoder for each mask. This can be prohibitively expensive for real-world applications. To address this problem, subsequent researchers propose to unify classification and segmentation within a shared space. Among them, SAN [60] designs a side-adaptor network to leverage CLIP features for reorganizing segmentation and classification. GKC [17] presents text-guided knowledge distillation strategy to transfer CLIP knowledge to specific classification layer. FCCLIP [62] proposes to leverage

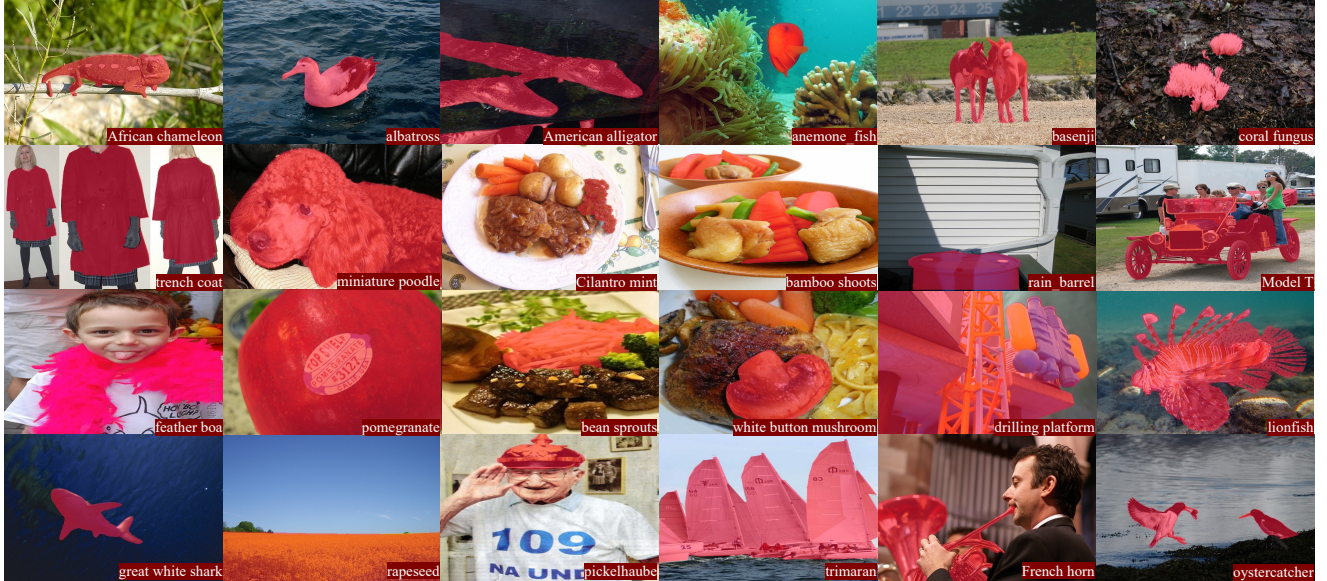


Figure 2. Illustration of the samples in the proposed OpenBench. Compared to existing test sets, our OpenBench has semantic categories that differ more from the training space, which helps to provide a more comprehensive measure of the model’s ability to perform open-vocabulary segmentation. The corresponding category name is labeled in the lower right corner of each image.

Table 1. Comparison of the statistics of our proposed OpenBench with existing datasets. ‘Cls’, ‘Img’, and ‘Sim’ indicate class, image, and similarity, respectively. ADE, PC, and VOC denote ADE20K [65], Pascal Context [44], and Pascal VOC [13]

| Dataset | Cls Num. | Img Num. | Mean Sim. | Median Sim. | Min Sim. | Max Sim. | Fine Granularity | Semantic Duplication |
|------------------|----------|----------|-----------|-------------|----------|----------|------------------|----------------------|
| VOC [13] | 20 | 1449 | 0.9756 | 1.0000 | 0.8449 | 1.0000 | × | × |
| PC-59 [44] | 59 | 5105 | 0.9481 | 1.0000 | 0.7658 | 1.0000 | × | × |
| ADE-150 [65] | 150 | 2000 | 0.8086 | 0.8228 | 0.1960 | 1.0000 | × | ✓ |
| Cityscapes [11] | 33 | 100 | 0.8488 | 0.8370 | 0.6746 | 1.0000 | × | × |
| PC-459 [44] | 459 | 5105 | 0.8374 | 0.8124 | 0.6718 | 1.0000 | ✓ | ✓ |
| ADE-847 [65] | 847 | 2000 | 0.7926 | 0.7913 | 0.1960 | 1.0000 | ✓ | ✓ |
| OpenBench (Ours) | 286 | 6056 | 0.6142 | 0.6452 | 0.2608 | 0.7947 | ✓ | × |

the local-awareness advantage of convolution backbones. Some works [10, 56] then discover that finetuning CLIP encoder could further enhance the model’s performance on existing test sets and develop effective one-stage framework.

However, we find that existing test sets are highly similar to the training set, which limits their ability to effectively evaluate the model’s comprehension of the open vocabulary semantics. Therefore, in this paper we propose a new benchmark OpenBench that is characterized by significant semantic differences from the training data. We also propose a method named OVSNet to improve the segmentation performance for diverse and open scenarios.

Vision-Language Pre-training. Vision-language pre-training aims to learn a unified visual-linguistic representation space. Early approaches [7, 28, 30, 40, 45, 47, 48, 64], constrained by small-scale datasets, struggle to achieve strong performance and require fine-tuning for downstream tasks. However, with the advent of large-scale web data,

recent works [23, 46] have demonstrated the benefits of leveraging such data to train a more robust multi-modal representation space. Among these, CLIP [46], the most widely used vision-language model, employs contrastive learning to link images with their corresponding captions, achieving impressive cross-modal alignment. Building upon previous works [12, 22, 27, 29, 59], we also utilize the well-aligned and generalized space of CLIP to enhance open-vocabulary segmentation.

3. Benchmark

3.1. Dataset Introduction

In Table 1, we present the statistics comparison of our proposed OpenBench with existing popular open-vocabulary segmentation datasets, including ADE-150 [65], ADE-847 [65], PC-59 [44], PC-459 [44], VOC [13], and Cityscapes [11]. Specifically, our OpenBench contains 286 categories, of which the maximum similarity to the train-

ing categories is 0.7947, the minimum is 0.2608, and the average similarity is 0.6142. It can be observed that, compared to existing datasets, our OpenBench exhibits a greater disparity from the training set, which better evaluates the model’s segmentation ability for arbitrary open categories.

Besides, our OpenBench contains fine-grained categories, *e.g.*, “oystercatcher”, rather than just generic broad category such as “bird” (corresponds to the “Fine Granularity” characterization in Table 1). This is important for evaluating whether the OVS models preserve the generalization capability of CLIP [46], which is inherently capable of detecting these fine-grained categories. Actually, PC-459 [44] and ADE-847 [65] also have fine-grained categories, but they suffer from semantic duplication problem. In detail, semantic duplication means that there will be both fine-grained categories as well as corresponding broad categories in these datasets, which would cause bias in the metrics calculation. For instance, if a model assigns the “door” tag to a region whose ground truth label is “double door”, it will be considered incorrect. For open-vocabulary segmentation setting, we argue that the responsibility of the model is to discern the correct semantic. The distribution of such duplication categories and the corresponding performance statistics is unreasonable. SCAN [37] also points similar observations and try to solve this by designing new metric. However, this requires manual judgment of the relationships between categories, introducing additional cost and uncertainty. Our OpenBench, on the other hand, has fine-grained semantics without the problem of semantic duplication, which helps to more accurately reflect the real capabilities of related models.

Figure 2 illustrates part of the categories contained in OpenBench, where some categories such as food related even differ significantly from the visual domain of the training set. Furthermore, our OpenBench also accounts for “other” or “background” pixels in images, which are often overlooked by existing datasets. This is important for open-vocabulary segmentation because the model is essentially forced to choose the most appropriate category from a predefined set. If there is no correct class and no “others” option in the candidate set, the model would be compelled to make an incorrect prediction. Moreover, “others” or “background” require the model to consider not only the direct visual-linguistic correspondence between the image content and each class, but also the relative relationships among different classes. This adds complexity and makes the task more relevant to real-world scenarios.

3.2. Dataset Collection

Our OpenBench is primarily derived from existing accessible segmentation datasets. To obtain semantic categories that differ significantly from the training set, *i.e.*, COCO [32], we first organize a group of segmen-

tation datasets that possess category annotations, *e.g.*, Food103 [53], Imagenet-S [14], and CamVid [3]. For all categories in the collected data, we leverage CLIP-L/14 [46] to compute their maximum similarity with COCO categories. Then we calculate the minimum similarity among the categories present in each image as the image’s similarity to the training semantics. If the image similarity is greater than the set threshold σ_1 , the image will be filtered. Conversely, if the similarity of the image is less than the threshold σ_1 , we would set the category exist in the image whose similarity is greater than the threshold σ_2 to “others” and save the related images and annotation. Finally, after manually filtering the categories for potential conflicts or duplicates, we get the OpenBench.

4. Method

4.1. Overview

The overall pipeline of our proposed OVSNet is shown in Figure 3. We leverage the vision and text encoder of pretrained CLIP [46] to encode the input image and category names, respectively. Then, a segmentation decoder is trained to decode the visual features, generating masks for potential targets and their corresponding query embeddings. We then leverage the predicted masks to extract related CLIP features with Mask Pooling operation. To integrate heterogeneous knowledge spaces and improve the representation robustness, Gradient-Free Aggregation fuses the query embeddings with pooled CLIP features. The aggregated visual embeddings are combined with linguistic embeddings to perform visual-linguistic alignment and generate final output. During training, a Proxy Calibration strategy is utilized to expand training space by applying supervision on the convex combination of training semantics.

4.2. Gradient-Free Aggregation

Although CLIP [46] exhibits strong generalization ability, it optimizes for image-level visual-linguistic alignment during pretraining, which creates a great domain gap compared to mask-level alignment. As a result, directly using CLIP features obtained through mask pooling for mask classification may lead to suboptimal performance. The query embeddings generated by the segmentation decoder, on the other hand, have a strong region-level alignment prior owing to their suitability for the training space. However, they struggle to recognize novel semantics.

Therefore, we propose to reorganize them to obtain more robust domain-adapted representations. An intuitive approach is to learn the intrinsic connection between them through self-attention or cross-attention mechanisms. However, we observe that such learning-based strategy tends to develop excessive reliance on query embeddings fitted to seen semantics during the training process while neglecting

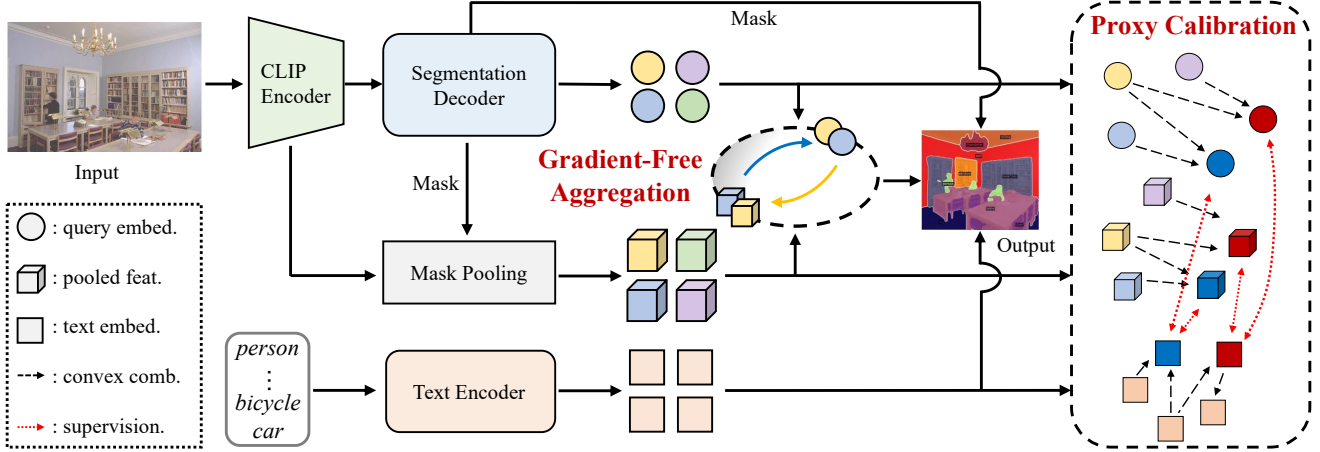


Figure 3. Pipeline of our OVSNet. The input image and corresponding categories are first encoded by pretrained CLIP [46]. A segmentation decoder is trained to decode the visual features and generate potential masks as well as corresponding query embeddings. We then leverage the predicted masks to extract related CLIP features with Mask Pooling operation. To integrate different knowledge spaces and improve the representation robustness, Gradient-Free Aggregation fuses the query embeddings with CLIP features. The aggregated visual embeddings are combined with class embeddings to perform visual-linguistic alignment and generate final output. During training, we apply Proxy Calibration strategy to expand training space in a cost-free manner.

the utilization of more generalizable information provided by CLIP, ultimately affecting the model’s ability to understand unlimited categories. Therefore, we propose to combine CLIP features and query embeddings via a gradient-free approach to avoid potential overfitting problems during the learning of the joint space. This is inspired by Random Walk algorithm [16]. Specifically, there are multiple iterations in this process where two features learn collaboratively in shared embedding space until convergence. Suppose we have N queries. For convenience, we omit the query index and take a random query as the example. The corresponding query embeddings and CLIP features can be represented by F_Q and F_C . F_Q and F_C are defined as the initial state F_Q^0 and F_C^0 at the 0-th iteration. Then we formulate affinity \mathcal{Z} by scaled dot product: $\mathcal{Z} = \lambda F_C^0 (F_Q^0)^\top$, where λ is the scaling factor. At t -th iteration, the query embedding F_Q^t is derived by the original embedding F_Q^0 and the updated CLIP feature F_C^{t-1} from previous iteration, which can be formulated as:

$$F_Q^t = \omega \text{Norm}(\mathcal{Z})^\top F_C^{t-1} + (1 - \omega) F_Q^0, \quad (1)$$

Subsequently, it is utilized to boost the CLIP feature of this iteration:

$$F_C^t = \omega \mathcal{Z} F_Q^t + (1 - \omega) F_C^0, \quad (2)$$

where $\omega \in (0, 1)$ is the factor that controls the degree of feature fusion. By combining the above equations we can obtain the overall iterative update formula of F_C^t :

$$F_C^t = (\omega^2 A)^t F_C^0 + (1 - \omega) \sum_{i=0}^{t-1} (\omega^2 A)^i (\omega \mathcal{Z} F_Q^0 + F_C^0), \quad (3)$$

where A denotes $\mathcal{Z} \text{Norm}(\mathcal{Z})^\top$. Moreover, to avoid the potential issue of unexpected gradient and simplify the calculation process, we use an approximate inference function based on Neumann Series [43] when $t \rightarrow \infty$. Then the update formula can be present as:

$$F_C^\infty = (1 - \omega)(I - \omega^2 A)^{-1}(\omega \mathcal{Z} F_Q^0 + F_C^0), \quad (4)$$

where I represents the identity matrix. With this gradient-free aggregation strategy, the model can recombine query embeddings with CLIP features to produce more robust region-level representations.

4.3. Proxy Calibration

A broader semantic training space tends to result in more generalized model representations. However, expanding the training space for OVS is costly due to the intensive prediction nature of segmentation tasks. To alleviate this problem, we propose a cost-free approach named Proxy Calibration (PC) to expand the training space and enhance the generalization ability of the model. It leverages the synthesis of proxy embeddings, which approximates novel semantics via convex combination between the in-vocabulary classes.

Specifically, having the aggregated query embeddings F_Q , we perform random convex combination of them during training to simulate embedding space for undefined classes, as shown by the black dotted line in Figure 3. This process can be formulated as:

$$F'_{Qmn} = \alpha * F_{Qm} + (1 - \alpha) * F_{Qn} \quad (5)$$

where $m, n \in \{1, 2, \dots, N\}$. α is a random weight sampled from the distribution of $\text{Beta}(\gamma, \gamma)$. F' denotes the gen-

Table 2. Performance comparison with state-of-the-art methods on existing benchmarks and the proposed OpenBench. ADE, PC, and VOC denote ADE20K [65], Pascal Context [44], and Pascal VOC [13], respectively. 171 and 133 indicate the number of training categories. * denotes the re-trained version according to the official code for fair comparison.

| Method | Training Dataset | ADE-150 | ADE-847 | PC-59 | PC-459 | VOC | OpenBench | Average Score |
|---------------------------|-------------------|-------------|-------------|-------------|-------------|-------------|-------------|---------------|
| Base-level CLIP Backbone | | | | | | | | |
| SimSeg* [59] | COCO-Stuff-171 | 21.1 | 6.9 | 51.9 | 9.7 | 91.8 | 19.4 | 33.5 |
| OVSeg [31] | COCO-Stuff-171 | 24.8 | 7.1 | 53.3 | 11.0 | 92.6 | 24.9 | 35.6 |
| SAN [60] | COCO-Stuff-171 | 27.5 | 10.1 | 53.8 | 12.6 | 94.0 | 39.6 | 39.6 |
| SCAN [37] | COCO-Stuff-171 | 30.8 | 10.8 | 58.4 | 13.2 | 97.0 | 38.7 | 41.5 |
| CATSeg [10] | COCO-Stuff-171 | 31.8 | 12.0 | 57.5 | 19.0 | 94.6 | 36.1 | 41.8 |
| SED [56] | COCO-Stuff-171 | 31.6 | 11.4 | 57.3 | 18.6 | 94.4 | 33.3 | 41.1 |
| FCCLIP* [62] | COCO-Panoptic-133 | 31.1 | 13.5 | 54.8 | 12.8 | 93.2 | 40.3 | 40.9 |
| MAFT [25] | COCO-Panoptic-133 | 29.1 | 10.1 | 53.5 | 12.8 | 90.0 | 37.5 | 38.8 |
| MAFT+ [26] | COCO-Panoptic-133 | 34.6 | 13.8 | 57.5 | 16.2 | 95.4 | 43.7 | 43.5 |
| OVSNet (Ours) | COCO-Panoptic-133 | 35.8 | 14.5 | 58.6 | 19.1 | 95.7 | 44.9 | 44.8 |
| Large-level CLIP Backbone | | | | | | | | |
| SimSeg* [59] | COCO-Stuff-171 | 21.7 | 7.1 | 52.2 | 10.2 | 92.3 | 27.8 | 35.2 |
| OVSeg [31] | COCO-Stuff-171 | 29.6 | 9.0 | 55.7 | 12.4 | 94.5 | 35.6 | 39.5 |
| SAN [60] | COCO-Stuff-171 | 32.1 | 12.4 | 57.7 | 15.7 | 94.6 | 43.4 | 42.7 |
| SCAN [37] | COCO-Stuff-171 | 33.5 | 14.0 | 59.3 | 16.3 | 97.1 | 49.4 | 44.9 |
| SED [56] | COCO-Stuff-171 | 35.2 | 13.9 | 60.6 | 22.6 | 96.1 | 45.6 | 45.6 |
| FCCLIP [62] | COCO-Panoptic-133 | 34.0 | 14.8 | 58.4 | 18.2 | 95.4 | 44.8 | 44.3 |
| MAFT [25] | COCO-Panoptic-133 | 34.4 | 13.1 | 57.5 | 17.0 | 93.0 | 41.7 | 42.8 |
| MAFT+ [26] | COCO-Panoptic-133 | 36.1 | 15.1 | 59.4 | 21.6 | 96.5 | 47.3 | 46.0 |
| OVSNet (Ours) | COCO-Panoptic-133 | 37.1 | 16.2 | 62.0 | 23.5 | 96.9 | 48.6 | 47.4 |

erated proxy embeddings. The same enhancement is performed for the corresponding CLIP feature F_C and linguistic embeddings F_T . Note that the text features here refer to the class representations of the ground truth regions corresponding to each query, which are obtained after Hungarian Matching [5]. Having the generated F'_Q , F'_C , and F'_T , we perform distance supervision on them to promote region-level visual-linguistic alignment performance from the perspective of proxy semantics. That is:

$$\mathcal{L}_{PQ} = 1 - \frac{\mathbf{F}'_Q \cdot \mathbf{F}'_T}{\|\mathbf{F}'_Q\|_2 \|\mathbf{F}'_T\|_2}, \quad (6)$$

$$\mathcal{L}_{PC} = 1 - \frac{\mathbf{F}'_C \cdot \mathbf{F}'_T}{\|\mathbf{F}'_C\|_2 \|\mathbf{F}'_T\|_2}, \quad (7)$$

where \mathcal{L}_{PQ} and \mathcal{L}_{PC} denote the applied proxy supervision for query embeddings and pooled CLIP features, respectively. The final proxy loss is the sum of \mathcal{L}_{PQ} and \mathcal{L}_{PC} . By applying additional supervision in this way, the model is not limited to a specific training space and can learn more robust visual representations.

5. Experiment

5.1. Evaluation Benchmark and Metric

To evaluate the effectiveness and generalization ability of our method on diverse scenarios, we conduct extensive experiments on the popular existing benchmarks, ADE20K150 [65], ADE20K847 [65], Pascal VOC [13], Pascal Context-59 [44], Pascal Context-459 [44] and our

proposed OpenBench. ADE20K is a large-scale scene understanding benchmark, containing 20k training images, 2k validation images, and 3k testing images. There are two splits of this dataset. ADE20K-150 contains 150 semantic classes whereas ADE20K-847 has 847 classes. The images of both are the same. Pascal Context is an extension of Pascal VOC 2010, containing 5,005 validation images. We take the commonly used PC-59 and challenging PC-459 version for validation. Pascal VOC contains 11,185 training images and 1,449 validation images from 20 classes. We use the provided augmented annotations. Following previous works [12, 15, 59], we take the *mean-intersection-over-union* (mIoU) as the metric to compare our model with previous state-of-the-art methods. In ablation, we assume the use of base-level CLIP as the backbone for comparison.

5.2. Implementation Details

We utilize the Mask2Former [8] as the segmentation decoder and the implementation is based on detectron2 [54]. The model is trained with batch size of 8 and total iteration of 60k. The base learning rate is 0.0001 with a polynomial schedule. Following previous works [26, 62], we take CLIP [46] of ConvNeXt as the backbone. The input image is resized and cropped to 1024×1024 . For data augmentation, random flip and color augmentation are adopted. The weight decay of the model is 0.05. λ and γ of GFA and PC are set to 0.2 and 2 by default. The segmentation loss consists of dice loss and cross entropy loss. The classification loss is cross entropy loss.

Table 3. Ablation experiments about the proposed methods. GFA and PC indicate the Gradient-Free Aggregation and Proxy Calibration strategies, respectively.

| Method | ADE-150 | PC-459 | OpenBench |
|----------|-------------|-------------|-------------|
| Baseline | 33.1 | 14.3 | 42.3 |
| + GFA | 34.7↑ (1.6) | 16.0↑ (1.7) | 43.7↑ (1.4) |
| + PC | 33.9↑ (0.8) | 17.2↑ (2.9) | 44.3↑ (2.0) |
| + Both | 35.8↑ (2.7) | 19.1↑ (4.8) | 44.9↑ (2.6) |

For the weights of the loss function, we set 5 and 2 for segmentation loss and classification loss, respectively. Other hyperparameters are the same as Mask2Former [9].

5.3. Main Results

We compare our model with existing state-of-the-art approaches in Table 2. It can be seen that with proxy calibration expanding training semantics and the gradient-free aggregation algorithm modeling the joint space, our model achieves the state-of-the-art performance on most popular benchmarks. *The last column counts the average performance across multiple datasets, which shows that our method performs well for both in-vocabulary as well as out-vocabulary diverse scenarios.* The relatively inferior performance of our method on VOC is due to the fact that the semantics of this dataset are almost contained in the training set, which tends to benefit models such as SCAN [37] that finetunes the CLIP backbone on training set. Besides, the greater divergence of OpenBench from training semantics does not imply that it is totally more challenging than other benchmarks, because the final performance is influenced by various factors such as image content complexity, image clarity, and the number of given categories. More discussion can be seen in the supplementary materials.

5.4. Ablation Study

Component Analysis Table 3 shows the ablations about the proposed Gradient-Free Aggregation (GFA) and Proxy Calibration (PC) strategy. We evaluate their effectiveness on both existing benchmarks and our proposed OpenBench. It can be seen that with GFA fusing CLIP feature and query embeddings, the model’s performance is greatly improved on both seen and unseen semantics. Besides, PC can facilitate the model’s ability to understand various scenarios by cost-free expansion of the training semantic space. When applying both, the model achieves the best performance.

Embedding Distribution Analysis To demonstrate that our proposed OpenBench is more open-vocabulary compared to the existing test sets, we perform t-SNE visualization of the category embeddings of the training set, the existing test sets, and our OpenBench in Figure 4. Besides, we also visualize the proxy embeddings generated by PC. We can see that the existing test sets (green dots) are overall similar to the training semantics (blue dots). Our Open-

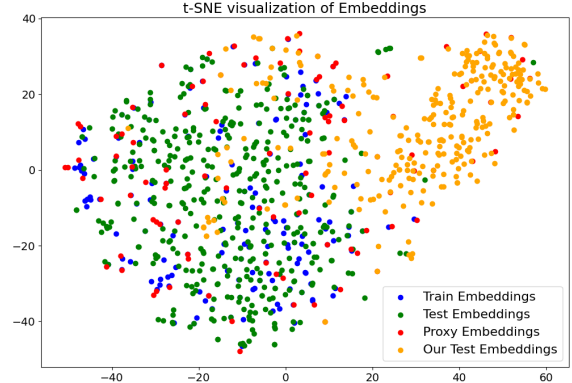


Figure 4. Visualization of category embeddings across the training space, existing evaluation space, our OpenBench space, and the generated proxy space.

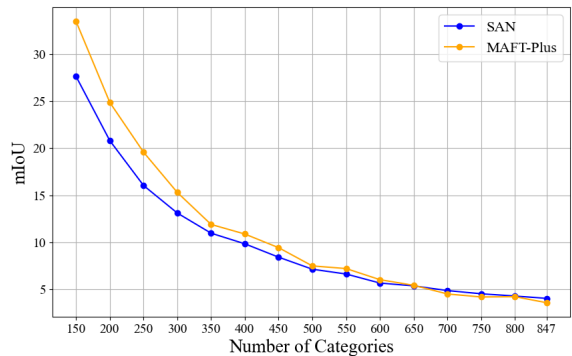


Figure 5. Impact of the number of inference categories on model performance. As the number of irrelevant categories increases, the model’s performance on the same image degrades.

Bench (orange dots), on the other hand, shows significant differences. In addition, the proxy embeddings (red dots) generated by PC expand the training set and thus help to improve the robustness and generalization of the model.

Analysis about Inference Class Number In this part we explore an interesting phenomenon: why the OVS models perform much worse on ADE-847 and PC-459 than on other test sets? Intuitively, this is because these datasets contain more novel categories. However, we find that another factor significantly impacts model performance, that is the number of categories fed into the model during inference. Let’s start with the conclusion: for the same model and test image, the model performance is worse when there are more inference categories given. In other words, the model may be able to make correct predictions when only a small number of categories are given. However, when more categories are prompted, the model’s output will be incorrect. Here we take two typical methods, SAN [60] and MAFT-Plus [26], as examples and show how their performance on the ADE-150 dataset changes as the number of categories increases. As shown in Figure 5, with the num-



Figure 6. Visualization of segmentation results. (a) - (d) demonstrate the successful segmentation cases of our method for seen and unseen categories. (e) and (f) display the adaptability for flexible text query. Best viewed in color.

ber of given irrelevant categories increases, the models of different technology routes show a consistent decline.

Internal Analysis of Proposed Strategies In Table 4 we conduct more experiments about the proposed methods. Specifically, we first compare our gradient-free aggregation designs with the typical learning-based feature fusion approaches in (a). Results show that vanilla attention performs inferior than our GFA, especially on the more open-vocabulary set OpenBench (degraded by more than 2.5 mIoU). This is because learning-based methods tend to develop a reliance on the segmentation query embeddings during training, while overlooking the CLIP features that inherently exhibit stronger generalization capabilities, thereby introducing biases.

We also experiment with the influence of different γ in Beta distribution to the performance of proxy calibration. The results are shown in Table 4 (b), where $\gamma = 1$ is equivalent to do not utilize PC. We find that different γ benefit the model performance while the performance is better when the intermediate probability density is high ($\gamma = 2$).

5.5. Visualization

Figure 6 shows some segmentation cases of our OVSNet. It can be seen that our method achieves excellent segmentation performance on various scenarios. Specifically, (a) - (d) demonstrate the excellent segmentation of our method for seen and unseen categories. (e) and (f) display the adapt-

Table 4. Ablation experiments within each modules. (a) shows the comparison of our gradient-free algorithm with learning-based method, *e.g.*, cross attention. (b) demonstrates the effect of γ of Beta distribution in the proxy learning strategy.

| | ADE-150 | PC-459 | OpenBench |
|---|--|--|--|
| <i>(a) Comparisons of GFA and learning-based strategy</i> | | | |
| Self Attn | 34.0 | 14.7 | 40.6 |
| Cross Attn | 34.2 | 14.8 | 41.2 |
| GFA | 34.7 | 16.0 | 43.7 |
| <i>(b) Effect of sampling distribution of PC</i> | | | |
| $\gamma = 1$ | 33.1 | 14.3 | 42.3 |
| $\gamma = 0.5$ | 33.6 \uparrow (0.5) | 16.1 \uparrow (1.8) | 43.7 \uparrow (1.4) |
| $\gamma = 2$ | 33.9\uparrow (0.8) | 17.2\uparrow (2.9) | 44.3\uparrow (2.0) |

ability for flexible text query, *e.g.*, change “building” to “opera house” and “car” to “ferrari”.

6. Conclusion

In this paper, we identify that the existing open-vocabulary segmentation evaluation sets suffer from excessive semantic similarity to the training set, which limits their ability to comprehensively assess the model’s open vocabulary understanding capabilities. To address this, we propose a new benchmark, OpenBench, which features significant differences from the training set and includes more fine-grained categories. Comparison on OpenBench further demonstrates that maintaining the generalization space of CLIP is crucial for OVS. Additionally, we introduce OVSNet, a method that leverages proxy calibration for cost-free

augmentation of the training space and gradient-free aggregation for fusing heterogeneous features. Experiments show that the proposed OVSNet achieves excellent performance on both existing datasets and the newly proposed OpenBench. We hope that our benchmark and model design could inspire further researches in this area.

References

- [1] Sule Bai, Yong Liu, Yifei Han, Haoji Zhang, and Yansong Tang. Self-calibrated clip for training-free open-vocabulary segmentation. *arXiv preprint arXiv:2411.15869*, 2024. 2
- [2] Sule Bai, Mingxing Li, Yong Liu, Jing Tang, Haoji Zhang, Lei Sun, Xiangxiang Chu, and Yansong Tang. Univg-r1: Reasoning guided universal visual grounding with reinforcement learning. *arXiv preprint arXiv:2505.14231*, 2025. 1
- [3] Gabriel J. Brostow, Jamie Shotton, Julien Fauqueur, and Roberto Cipolla. Segmentation and recognition using structure from motion point clouds. In *ECCV*, pages 44–57, 2008. 4
- [4] Maxime Bucher, Tuan-Hung Vu, Matthieu Cord, and Patrick Pérez. Zero-shot semantic segmentation. In *NeurIPS*, 2019. 2
- [5] Nicolas Carion, Francisco Massa, Gabriel Synnaeve, Nicolas Usunier, Alexander Kirillov, and Sergey Zagoruyko. End-to-end object detection with transformers. In *ECCV*, 2020. 6
- [6] Liang-Chieh Chen, George Papandreou, Iasonas Kokkinos, Kevin Murphy, and Alan L. Yuille. Deeplab: Semantic image segmentation with deep convolutional nets, atrous convolution, and fully connected crfs. *TPAMI*, 2018. 1
- [7] Yen-Chun Chen, Linjie Li, Licheng Yu, Ahmed El Kholy, Faisal Ahmed, Zhe Gan, Yu Cheng, and Jingjing Liu. UNITER: learning universal image-text representations. *arXiv preprint arXiv:1909.11740*, 2019. 3
- [8] Bowen Cheng, Anwesa Choudhuri, Ishan Misra, Alexander Kirillov, Rohit Girdhar, and Alexander G. Schwing. Mask2former for video instance segmentation. *arXiv preprint arXiv:2112.10764*, 2021. 6
- [9] Bowen Cheng, Ishan Misra, Alexander G. Schwing, Alexander Kirillov, and Rohit Girdhar. Masked-attention mask transformer for universal image segmentation. In *CVPR*, 2022. 7
- [10] Seokju Cho, Heeseong Shin, Sunghwan Hong, Anurag Arnab, Paul Hongsuck Seo, and Seungryong Kim. Cat-seg: Cost aggregation for open-vocabulary semantic segmentation. In *CVPR*, pages 4113–4123, 2024. 1, 2, 3, 6
- [11] Marius Cordts, Mohamed Omran, Sebastian Ramos, Timo Rehfeld, Markus Enzweiler, Rodrigo Benenson, Uwe Franke, Stefan Roth, and Bernt Schiele. The cityscapes dataset for semantic urban scene understanding. In *CVPR*, 2016. 3
- [12] Jian Ding, Nan Xue, Gui-Song Xia, and Dengxin Dai. Decoupling zero-shot semantic segmentation. In *CVPR*, 2022. 1, 2, 3, 6
- [13] Mark Everingham, SM Ali Eslami, Luc Van Gool, Christopher KI Williams, John Winn, and Andrew Zisserman. The pascal visual object classes challenge: A retrospective. *IJCV*, 111:98–136, 2015. 2, 3, 6
- [14] Shanghua Gao, Zhong-Yu Li, Ming-Hsuan Yang, Ming-Ming Cheng, Junwei Han, and Philip Torr. Large-scale unsupervised semantic segmentation. *TPAMI*, 45(6):7457–7476, 2022. 4
- [15] Golnaz Ghiasi, Xiuye Gu, Yin Cui, and Tsung-Yi Lin. Open-vocabulary image segmentation. *arXiv preprint arXiv:2112.12143*, 2021. 1, 2, 6
- [16] Leo Grady. Random walks for image segmentation. *IEEE TPAMI*, 28(11):1768–1783, 2006. 2, 5
- [17] Kunyang Han, Yong Liu, Jun Hao Liew, Henghui Ding, Jijun Liu, Yitong Wang, Yansong Tang, Yujiu Yang, Jiashi Feng, Yao Zhao, et al. Global knowledge calibration for fast open-vocabulary segmentation. In *Proceedings of the IEEE/CVF International Conference on Computer Vision*, pages 797–807, 2023. 1, 2
- [18] Shuting He, Henghui Ding, and Wei Jiang. Primitive generation and semantic-related alignment for universal zero-shot segmentation. In *CVPR*, 2023. 1
- [19] Yihan Hu, Jiazhi Yang, Li Chen, Keyu Li, Chonghao Sima, Xizhou Zhu, Siqi Chai, Senyao Du, Tianwei Lin, Wenhui Wang, et al. Planning-oriented autonomous driving. In *Proceedings of the IEEE/CVF Conference on Computer Vision and Pattern Recognition*, pages 17853–17862, 2023. 1
- [20] Jiaqi Huang, Zunnan Xu, Ting Liu, Yong Liu, Haonan Han, Kehong Yuan, and Xiu Li. Densely connected parameter-efficient tuning for referring image segmentation. *arXiv preprint arXiv:2501.08580*, 2025. 1
- [21] Xiaoke Huang, Jianfeng Wang, Yansong Tang, Zheng Zhang, Han Hu, Jiwen Lu, Lijuan Wang, and Zicheng Liu. Segment and caption anything. *arXiv preprint arXiv:2312.00869*, 2023. 1
- [22] Joonhyun Jeong, Geondo Park, Jayeon Yoo, Hyungsik Jung, and Heesu Kim. Proxydet: Synthesizing proxy novel classes via classwise mixup for open-vocabulary object detection. In *AAAI*, pages 2462–2470, 2024. 3
- [23] Chao Jia, Yinfei Yang, Ye Xia, Yi-Ting Chen, Zarana Parekh, Hieu Pham, Quoc V. Le, Yun-Hsuan Sung, Zhen Li, and Tom Duerig. Scaling up visual and vision-language representation learning with noisy text supervision. In *ICML*, 2021. 3
- [24] Chao Jia, Yinfei Yang, Ye Xia, Yi-Ting Chen, Zarana Parekh, Hieu Pham, Quoc Le, Yun-Hsuan Sung, Zhen Li, and Tom Duerig. Scaling up visual and vision-language representation learning with noisy text supervision. In *ICML*, pages 4904–4916, 2021. 1
- [25] Siyu Jiao, Yunchao Wei, Yaowei Wang, Yao Zhao, and Humphrey Shi. Learning mask-aware clip representations for zero-shot segmentation. *arXiv preprint arXiv:2310.00240*, 2023. 1, 6
- [26] Siyu Jiao, Hongguang Zhu, Jiannan Huang, Yao Zhao, Yunchao Wei, and Humphrey Shi. Collaborative vision-text representation optimizing for open-vocabulary segmentation. In *ECCV*, pages 399–416, 2025. 6, 7
- [27] Boyi Li, Kilian Q. Weinberger, Serge J. Belongie, Vladlen Koltun, and René Ranftl. Language-driven semantic segmentation. In *ICLR*, 2022. 1, 3
- [28] Gen Li, Nan Duan, Yuejian Fang, Ming Gong, and Daxin Jiang. Unicoder-vl: A universal encoder for vision and language by cross-modal pre-training. In *AAAI*, 2020. 3

- [29] Wanhua Li, Xiaoke Huang, Zheng Zhu, Yansong Tang, Xiu Li, Jie Zhou, and Jiwen Lu. Ordinalclip: Learning rank prompts for language-guided ordinal regression. *NeurIPS*, pages 35313–35325, 2022. 3
- [30] Xiujun Li, Xi Yin, Chunyuan Li, Pengchuan Zhang, Xiaowei Hu, Lei Zhang, Lijuan Wang, Houdong Hu, Li Dong, Furu Wei, Yejin Choi, and Jianfeng Gao. Oscar: Object-semantics aligned pre-training for vision-language tasks. In *ECCV*, 2020. 3
- [31] Feng Liang, Bichen Wu, Xiaoliang Dai, Kunpeng Li, Yinan Zhao, Hang Zhang, Peizhao Zhang, Peter Vajda, and Diana Marculescu. Open-vocabulary semantic segmentation with mask-adapted CLIP. *arXiv preprint arXiv:2210.04150*, 2022. 1, 2, 6
- [32] Tsung-Yi Lin, Michael Maire, Serge J. Belongie, James Hays, Pietro Perona, Deva Ramanan, Piotr Dollár, and C. Lawrence Zitnick. Microsoft COCO: common objects in context. In *ECCV*, 2014. 4
- [33] Yong Liu, Ran Yu, Xinyuan Zhao, and Yujiu Yang. Quality-aware and selective prior enhancement memory network for video object segmentation. In *CVPR Workshop*, 2021. 1
- [34] Yong Liu, Ran Yu, Jiahao Wang, Xinyuan Zhao, Yitong Wang, Yansong Tang, and Yujiu Yang. Global spectral filter memory network for video object segmentation. In *ECCV*, pages 648–665, 2022.
- [35] Yong Liu, Ran Yu, Fei Yin, Xinyuan Zhao, Wei Zhao, Weihao Xia, and Yujiu Yang. Learning quality-aware dynamic memory for video object segmentation. In *ECCV*, pages 468–486, 2022.
- [36] Yong Liu, Cairong Zhang, Yitong Wang, Jiahao Wang, Yujiu Yang, and Yansong Tang. Universal segmentation at arbitrary granularity with language instruction. *arXiv preprint arXiv:2312.01623*, 2023. 1
- [37] Yong Liu, Sule Bai, Guanbin Li, Yitong Wang, and Yansong Tang. Open-vocabulary segmentation with semantic-assisted calibration. In *CVPR*, pages 3491–3500, 2024. 1, 4, 6, 7
- [38] Yong Liu, Ran Yu, Fei Yin, Xinyuan Zhao, Wei Zhao, Weihao Xia, Jiahao Wang, Yitong Wang, Yansong Tang, and Yujiu Yang. Learning high-quality dynamic memory for video object segmentation. *IEEE TPAMI*, 2025. 1
- [39] Guanxing Lu, Ziwei Wang, Changliu Liu, Jiwen Lu, and Yansong Tang. Thinkbot: Embodied instruction following with thought chain reasoning. *arXiv preprint arXiv:2312.07062*, 2023. 1
- [40] Jiasen Lu, Dhruv Batra, Devi Parikh, and Stefan Lee. Vilbert: Pretraining task-agnostic visiolinguistic representations for vision-and-language tasks. In *NeurIPS*, 2019. 3
- [41] Zhuoyan Luo, Yicheng Xiao, Yong Liu, Shuyan Li, Yitong Wang, Yansong Tang, Xiu Li, and Yujiu Yang. Soc: Semantic-assisted object cluster for referring video object segmentation. *arXiv preprint arXiv:2305.17011*, 2023. 2
- [42] Zhuoyan Luo, Yinghao Wu, Yong Liu, Yicheng Xiao, Xiaoping Zhang, and Yujiu Yang. Hdc: Hierarchical semantic decoding with counting assistance for generalized referring expression segmentation. *arXiv preprint arXiv:2405.15658*, 2024. 1
- [43] Carl D Meyer and Ian Stewart. *Matrix analysis and applied linear algebra*. SIAM, 2023. 5
- [44] Roozbeh Mottaghi, Xianjie Chen, Xiaobai Liu, Nam-Gyu Cho, Seong-Whan Lee, Sanja Fidler, Raquel Urtasun, and Alan L. Yuille. The role of context for object detection and semantic segmentation in the wild. In *CVPR*, 2014. 2, 3, 4, 6
- [45] Mengxue Qu, Yu Wu, Wu Liu, Qiqi Gong, Xiaodan Liang, Olga Russakovsky, Yao Zhao, and Yunchao Wei. Siri: A simple selective retraining mechanism for transformer-based visual grounding. In *ECCV*, 2022. 3
- [46] Alec Radford, Jong Wook Kim, Chris Hallacy, Aditya Ramesh, Gabriel Goh, Sandhini Agarwal, Girish Sastry, Amanda Askell, Pamela Mishkin, Jack Clark, Gretchen Krueger, and Ilya Sutskever. Learning transferable visual models from natural language supervision. In *ICML*, 2021. 1, 2, 3, 4, 5, 6
- [47] Yiqin Wang, Haoji Zhang, Yansong Tang, Yong Liu, Jiashi Feng, Jifeng Dai, and Xiaoje Jin. Hierarchical memory for long video qa. *arXiv preprint arXiv:2407.00603*, 2024. 3
- [48] Yulin Wang, Haoji Zhang, Yang Yue, Shiji Song, Chao Deng, Junlan Feng, and Gao Huang. Uni-adafocus: Spatial-temporal dynamic computation for video recognition. *IEEE TPAMI*, 2024. 3
- [49] Yuji Wang, Jingchen Ni, Yong Liu, Chun Yuan, and Yansong Tang. Iterprime: Zero-shot referring image segmentation with iterative grad-cam refinement and primary word emphasis. In *AAAI*, pages 8159–8168, 2025. 1
- [50] Yuji Wang, Haoran Xu, Yong Liu, Jiaze Li, and Yansong Tang. Sam2-love: Segment anything model 2 in language-aided audio-visual scenes. In *CVPR*, pages 28932–28941, 2025.
- [51] Cong Wei, Yujie Zhong, Haoxian Tan, Yong Liu, Zheng Zhao, Jie Hu, and Yujiu Yang. Hyperseg: Towards universal visual segmentation with large language model. *arXiv preprint arXiv:2411.17606*, 2024.
- [52] Cong Wei, Yujie Zhong, Haoxian Tan, Yingsen Zeng, Yong Liu, Zheng Zhao, and Yujiu Yang. Instructseg: Unifying instructed visual segmentation with multi-modal large language models. *arXiv preprint arXiv:2412.14006*, 2024. 1
- [53] Xiongwei Wu, Xin Fu, Ying Liu, Ee-Peng Lim, Steven CH Hoi, and Qianru Sun. A large-scale benchmark for food image segmentation. In *ACM MM*, 2021. 4
- [54] Yuxin Wu, Alexander Kirillov, Francisco Massa, Wan-Yen Lo, and Ross Girshick. Detectron2. <https://github.com/facebookresearch/detectron2>, 2019. 6
- [55] Yongqin Xian, Subhabrata Choudhury, Yang He, Bernt Schiele, and Zeynep Akata. Semantic projection network for zero- and few-label semantic segmentation. In *CVPR*, 2019. 1, 2
- [56] Bin Xie, Jiale Cao, Jin Xie, Fahad Shahbaz Khan, and Yanwei Pang. Sed: A simple encoder-decoder for open-vocabulary semantic segmentation. In *CVPR*, pages 3426–3436, 2024. 1, 2, 3, 6
- [57] Enze Xie, Wenhai Wang, Zhiding Yu, Anima Anandkumar, Jose M. Alvarez, and Ping Luo. Segformer: Simple and efficient design for semantic segmentation with transformers. In *NIPS*, 2021. 1

- [58] Jiarui Xu, Sifei Liu, Arash Vahdat, Wonmin Byeon, Xiaolong Wang, and Shalini De Mello. Open-vocabulary panoptic segmentation with text-to-image diffusion models. In *CVPR*, pages 2955–2966, 2023. [2](#)
- [59] Mengde Xu, Zheng Zhang, Fangyun Wei, Yutong Lin, Yue Cao, Han Hu, and Xiang Bai. A simple baseline for zero-shot semantic segmentation with pre-trained vision-language model. *arXiv preprint arXiv:2112.14757*, 2021. [1](#), [2](#), [3](#), [6](#)
- [60] Mengde Xu, Zheng Zhang, Fangyun Wei, Han Hu, and Xiang Bai. Side adapter network for open-vocabulary semantic segmentation. In *CVPR*, pages 2945–2954, 2023. [1](#), [2](#), [6](#), [7](#)
- [61] Xin Xu, Tianyi Xiong, Zheng Ding, and Zhuowen Tu. Masq-clip for open-vocabulary universal image segmentation. In *ICCV*, pages 887–898, 2023. [1](#)
- [62] Qihang Yu, Ju He, Xueqing Deng, Xiaohui Shen, and Liang-Chieh Chen. Convolutions die hard: Open-vocabulary segmentation with single frozen convolutional clip. *NeurIPS*, pages 32215–32234, 2023. [1](#), [2](#), [6](#)
- [63] Hui Zhang and Henghui Ding. Prototypical matching and open set rejection for zero-shot semantic segmentation. In *ICCV*, 2021. [1](#)
- [64] Haoji Zhang, Yiqin Wang, Yansong Tang, Yong Liu, Jiashi Feng, Jifeng Dai, and Xiaojie Jin. Flash-vstream: Memory-based real-time understanding for long video streams. *arXiv preprint arXiv:2406.08085*, 2024. [3](#)
- [65] Bolei Zhou, Hang Zhao, Xavier Puig, Sanja Fidler, Adela Barriuso, and Antonio Torralba. Scene parsing through ADE20K dataset. In *CVPR*, 2017. [2](#), [3](#), [4](#), [6](#)